

Available online at [www.sciencedirect.com](http://www.sciencedirect.com)**ScienceDirect**

Nuclear Physics B 897 (2015) 821–831

[www.elsevier.com/locate/nuclphysb](http://www.elsevier.com/locate/nuclphysb)

# Modulation, asymmetry and the diurnal variation in axionic dark matter searches

Y. Semertzidis<sup>a,b</sup>, J.D. Vergados<sup>a,b,\*</sup><sup>a</sup> KAIST University, Daejeon, Republic of Korea<sup>b</sup> Center for Axion and Precision Physics Research, IBS, Daejeon 305-701, Republic of Korea

Received 21 February 2015; received in revised form 21 April 2015; accepted 15 June 2015

Available online 22 June 2015

Editor: Hong-Jian He

---

## Abstract

In the present work we study possible time dependent effects in Axion Dark Matter searches employing resonant cavities. We find that the width of the resonance, which depends on the axion mean square velocity in the local frame, will show an annual variation due to the motion of the Earth around the sun (modulation). Furthermore, if the experiments become directional, employing suitable resonant cavities, one expects large asymmetries in the observed widths relative to the sun's direction of motion. Due to the rotation of the Earth around its axis, these asymmetries will manifest themselves as a diurnal variation in the observed width. © 2015 The Authors. Published by Elsevier B.V. This is an open access article under the CC BY license (<http://creativecommons.org/licenses/by/4.0/>). Funded by SCOAP<sup>3</sup>.

---

## 1. Introduction

The axion has been proposed a long time ago as a solution to the strong CP problem [1] resulting to a pseudo Goldstone Boson [2–6], but it has also been recognized as a prominent dark matter candidate [7]. In fact, realizing an idea proposed a long time ago by Sikivie [8], various experiments such as ADMX and ADMX-HF collaborations [9–12] are now planned to search for them. In addition, the newly established center for axion and physics research (CAPP) has started an ambitious axion dark matter research program [13], using SQUID and HFET

---

\* Corresponding author at: Center for Axion and Precision Physics Research, IBS, Daejeon 305-701, Republic of Korea.

E-mail address: [vergados@uoi.gr](mailto:vergados@uoi.gr) (J.D. Vergados).

<http://dx.doi.org/10.1016/j.nuclphysb.2015.06.014>

0550-3213/© 2015 The Authors. Published by Elsevier B.V. This is an open access article under the CC BY license (<http://creativecommons.org/licenses/by/4.0/>). Funded by SCOAP<sup>3</sup>.

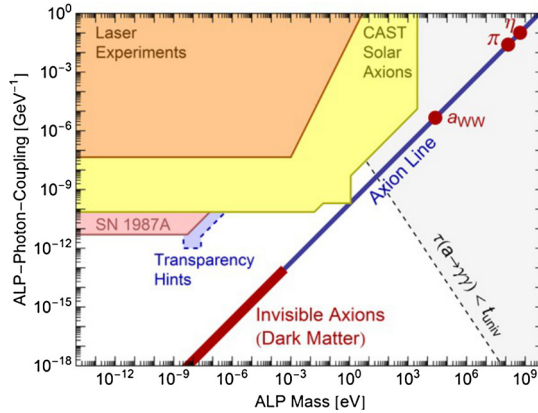


Fig. 1. The parameter space for axion like particles (courtesy of professor Raffelt).

technologies [14]. The allowed parameter space has been presented in a nice slide by Raffelt [15] in the recent Multidark-IBS workshop. From Fig. 1 containing information for all the axion like particles, we are interested in the regime allowed for invisible axions, which can be dark matter candidates.

In the present work we will take the view that the axion is non-relativistic with mass in  $\mu\text{eV}$ – $\text{meV}$  scale moving with an average velocity which is  $\approx 0.8 \times 10^{-3} c$ . The width of the observed resonance depends on the axion mean square velocity in the local frame. Thus one expects it to exhibit a time variation due to the motion of the Earth. Furthermore in directional experiments involving long cavities, one expects asymmetries with regard to the sun’s direction of motion as it goes around the center of the galaxy. Due to the rotation of the Earth around its axis these asymmetries in the width of the resonance will manifest themselves in their diurnal variation. These two special signatures, expected to be sizable, may aid the analysis of axion dark searches in discriminating against possible backgrounds.

## 2. Brief summary of the formalism

The photon axion interaction is dictated by the Lagrangian:

$$\mathcal{L}_{a\gamma\gamma} = g_{a\gamma\gamma} a \mathbf{E} \cdot \mathbf{B}, \quad g_{a\gamma\gamma} = \frac{\alpha g_\gamma}{\pi f_a}, \tag{2.1}$$

where  $\mathbf{E}$  and  $\mathbf{B}$  are the electric and magnetic fields,  $g_\gamma$  a model dependent constant on order one [9,16,17] and  $f_a$  the axion decay constant. Axion dark matter detectors [16] employ an external magnetic field,  $\mathbf{B} \rightarrow \mathbf{B}_0$  in the previous equation, in which case one of the photons is replaced by a virtual photon, while the other maintains the energy of the axion, which is its mass plus a small fraction of kinetic energy.

The power produced, see e.g. [9], is given by:

$$P_{mnp} = g_{a\gamma\gamma}^2 \frac{\rho_a}{m_a} B_0^2 V C_{mnp} Q_L \tag{2.2}$$

$Q_L$  is the loaded quality factor of the cavity. Here we have assumed  $Q_L$  is smaller than the axion width  $Q_a$ , see below. More generally,  $Q_L$  should be substituted by  $\min(Q_L, Q_a)$ . This power depends on the axion density and is pretty much independent of the velocity distribution.

The axion power spectrum, which is of great interest to experiments, is written as a Breit-Wigner shape [16,18]:

$$|A(\omega)|^2 = \frac{\rho_D}{m_a^2} \frac{\Gamma}{(\omega - \omega_a)^2 + (\Gamma/2)^2}, \quad \Gamma = \frac{\omega_a}{Q_a} \tag{2.3}$$

with  $\omega_a = m_a (1 + (1/6) \langle v^2 \rangle)$  and  $Q_a = m_a / (m_a \langle v^2 \rangle / 3)$ . The width explicitly depends on the average axion velocity squared in the laboratory. Thus the width in the laboratory is affected by the sun’s motion. In the non-directional experiments  $\langle v^2 \rangle = (3/2)v_0^2$  becomes  $\langle v^2 \rangle = (5/2)v_0^2$  ( $v_0$  the velocity of the sun around the center of the galaxy). If we take into account the motion of the Earth around the sun the width becomes time dependent (modulation) as described below (see Section 3.2).

The situation becomes more dramatic as soon the experiment is directional. In this case the width depends strongly on the direction of observation relative to the sun’s direction of motion. Directional experiments can, in principle, be performed by changing the orientation of a long cavity [9,19,20], provided that the axion wavelength is not larger than the length of the cylinder,  $\lambda_a \leq h$ . In the ADMX [9] experiment  $h = 100$  cm, while from their Fig. 3 one can see that the relevant for dark matter wavelengths  $\lambda_a$  are between 1 and 65 cm.

### 3. Modification of the width due to the motion of the Earth and the sun

From the above discussion it appears that velocity distribution of axions may play a role in the experiments.

#### 3.1. The velocity distribution

If the axion is going to be considered as dark matter candidate, its density should fit the rotational curves. Thus for temperatures  $T$  such that  $m_a/T \approx 4 \times 10^6$  the velocity distribution can be taken to be analogous to that assumed for WIMPs, i.e. an M–B distribution with a characteristic velocity which equals the velocity of the sun around the center of the galaxy, i.e.  $v_0 \approx 220$  km/s. So we will employ the distribution:

$$f(\vec{v}) = \frac{1}{(\sqrt{\pi} v_0)^3} e^{-\frac{v^2}{v_0^2}} \tag{3.4}$$

In order to compute the average of the velocity squared entering the power spectrum we need to find the local velocity distribution by taking into account the velocity of the Earth around the sun and the velocity of the sun around the center of the galaxy. The first motion leads to a time dependence of the observed signal in standard experiments, while the latter motion leads to asymmetries in directional experiments.

#### 3.2. The annual modulation in non-directional experiments

The modification of the velocity distribution in the local frame due to annual motion of the Earth is expected to affect the detection of axions in a time dependent way, which, following the terminology of the standard WIMPs, will be called the modulation effect [21] (the corresponding effect due to the rotation of the Earth around its own axis is too small to be observed). Periodic signatures for the detection of cosmic axions were first considered by Turner [22].

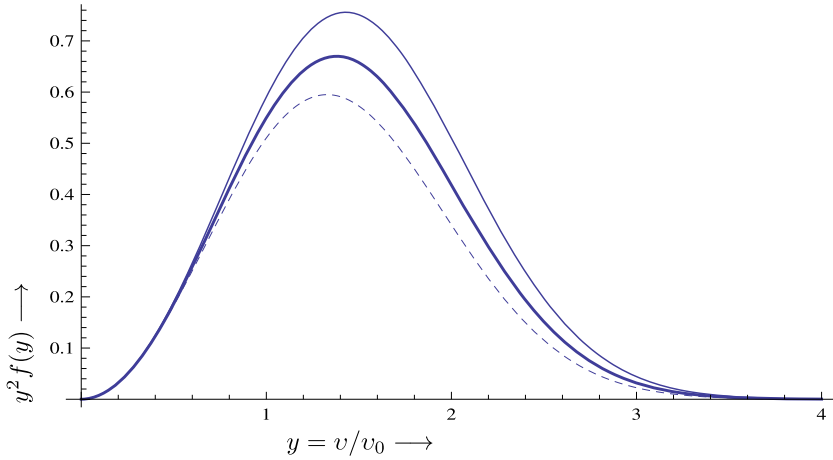


Fig. 2. The axion velocity distribution in the local frame. It is changing with time due to the motion of the Earth and the sun. We exhibit here the distribution in June (solid line), in December (thick solid line) and in September or March (dotted line). The last curve coincides with that in which the motion of the Earth is ignored.

So our next task is to transform the velocity distribution from the galactic to the local frame. The needed equation, see e.g. [23], is:

$$\mathbf{y} \rightarrow \mathbf{y} + \hat{v}_s + \delta (\sin \alpha \hat{x} - \cos \alpha \cos \gamma \hat{y} + \cos \alpha \sin \gamma \hat{v}_s), \quad y = \frac{v}{v_0} \tag{3.5}$$

with  $\gamma \approx \pi/6$ ,  $\hat{v}_s$  a unit vector in the Sun’s direction of motion,  $\hat{x}$  a unit vector radially out of the galaxy in our position and  $\hat{y} = \hat{v}_s \times \hat{x}$ . The last term in the first expression of Eq. (3.5) corresponds to the motion of the Earth around the Sun with  $\delta$  being the ratio of the modulus of the Earth’s velocity around the Sun divided by the Sun’s velocity around the center of the Galaxy, i.e.  $v_0 \approx 220$  km/s and  $\delta \approx 0.135$ . The above formula assumes that the motion of both the Sun around the Galaxy and of the Earth around the Sun are uniformly circular. The exact orbits are, of course, more complicated but such deviations are not expected to significantly modify our results. In Eq. (3.5)  $\alpha$  is the phase of the Earth ( $\alpha = 0$  around the beginning of June).<sup>1</sup>

The velocity distribution in the local frame is affected by the motion of the Earth as exhibited in Fig. 2 at four characteristic periods. The ratio of the modulated width divided by that obtained by ignoring the local velocity, as a function of the phase of the Earth, is shown in Fig. 3. More appropriate in the analysis of the experiments is the relative modulated width, i.e. the ratio of the time dependent width divided by the time averaged with, is shown in Fig. 4. The results shown here are for spherically symmetric M–B distribution as well as an axially symmetric one with asymmetry parameter  $\beta = 0.5$  with

$$\beta = 1 - \frac{\langle v_r^2 \rangle}{2 \langle v_t^2 \rangle} \tag{3.6}$$

with  $v_r$  the radial, i.e. radially out of the galaxy, and  $v_t$  the tangential component of the velocity. Essentially similar results are obtained by more exotic models, like a combination of M–B and

<sup>1</sup> One could, of course, make the time dependence of the rates due to the motion of the Earth more explicit by writing  $\alpha \approx (6/5)\pi (2(t/T) - 1)$ , where  $t/T$  is the fraction of the year.

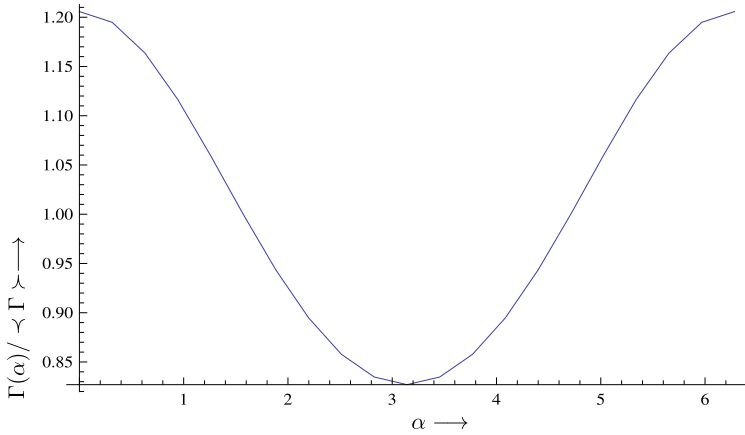


Fig. 3. The ratio of the modulated width divided by that expected if the motion of the sun and the Earth is ignored, as a function of the phase of the Earth.

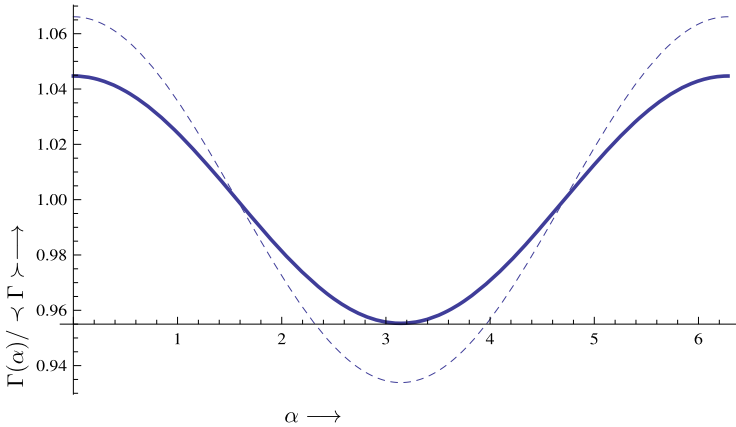


Fig. 4. The ratio of the modulated width divided by the time averaged width as a function of the phase of the Earth. The solid line corresponds to the standard M–B distribution and the dotted line to an axially symmetric M–B distribution with asymmetry parameter  $\beta = 0.5$  (see text).

Debris flows considered by Spergel and collaborators [24]. We see that the effect is small, around 15% difference between maximum and minimum in the presence of the asymmetry, but still larger than that expected in ordinary dark matter searches. If we do detect the axion frequency, then we can determine its width with high accuracy and detect its modulation as a function of time.

### 3.3. Asymmetry of the rates in directional experiments

Consideration of the velocity distribution will give an important signature, if directional experiments become feasible. This can be seen as follows:

- The width will depend specified by two angles  $\Theta$  and  $\Phi$ .  
The angle  $\Theta$  is the polar angle between the sun’s velocity and the direction of observation.

The angle  $\Phi$  is measured in a plane perpendicular to the sun’s velocity, starting from the line coming radially out of the galaxy and passing through the sun’s location.

- The axion velocity, in units of the solar velocity, is given as

$$\mathbf{y} = y \left( \hat{x} \sqrt{1 - \xi^2} \cos \phi + \hat{y} \sqrt{1 - \xi^2} \sin \phi + \hat{z} \xi \right) \tag{3.7}$$

- Set  $\delta = 0$ , i.e. ignore the motion of the Earth around the sun.

Then the velocity distribution in the local frame is obtained by the substitution:

$$v^2 \rightarrow v_0^2 \left( y^2 + 1 + 2y \left( \xi \cos \Theta + \sqrt{1 - \xi^2} \sin \Theta (\cos \Phi \cos \phi + \sin \Phi \sin \phi) \right) \right) \tag{3.8}$$

One then can integrate over  $\xi$  and  $\phi$ . The results become essentially independent of  $\Phi$ , so long as the motion of the Earth around the sun is ignored.<sup>2</sup> Thus we obtain  $\langle v^2 \rangle$  from the axion velocity distribution for various polar angles  $\Theta$ .

We write the width observed in a directional experiment as:

$$\Gamma = r(\Theta) \Gamma_{st} \tag{3.9}$$

where  $\Gamma_{st}$  is the width in the standard experiments. Ignoring the motion of the Earth around the sun the factor  $r$  depends only on  $\Theta$ . Furthermore, if for simplicity we ignore the upper velocity bound (cut off) in the M–B distribution, i.e. the escape velocity  $v_{esc} = 2.84v_0$ , we can get the solution in analytic form. We find:

$$r(\Theta) = \frac{2}{5} \frac{e^{-1}}{2} \left( e^{\cos^2 \Theta} (\cos 2\Theta + 4) \operatorname{erfc}(\cos \Theta) - \frac{2 \cos \Theta}{\sqrt{\pi}} \right), \text{ (sense known)} \tag{3.10}$$

where

$$\operatorname{erfc}(z) = 1 - \operatorname{erf}(z), \operatorname{erf}(z) = \int_0^z dt e^{-t^2} \text{ (error function).}$$

$$r(\Theta) = \frac{2}{5} \frac{1}{2} e^{-\sin^2 \Theta} (\cos 2\Theta + 4), \text{ (sense of direction not known)} \tag{3.11}$$

The adoption of an upper cut off has little effect. In Fig. 5 we present the exact results. The above results were obtained with an M–B velocity distribution.<sup>3</sup>

Our results indicate that the width will exhibit diurnal variation! For a cylinder of Length  $L$  such a variation is expected to be favored [20] in the regime of  $m_a L = 10\text{--}25 \times 10^{-4}$  eV m. This diurnal variation will be discussed in the next section.

<sup>2</sup> The annual modulation of the expected results due to the motion of the Earth around the sun will show up in the directional experiments as well, but it is going to be less important and it will not be discussed here.

<sup>3</sup> Evaluation of the relevant average velocity squared in some other models [25,26], which lead to caustic ring distributions, can also be worked out for axions as above in a fashion analogous to that of WIMPs [27], but this is not the subject of the present paper.

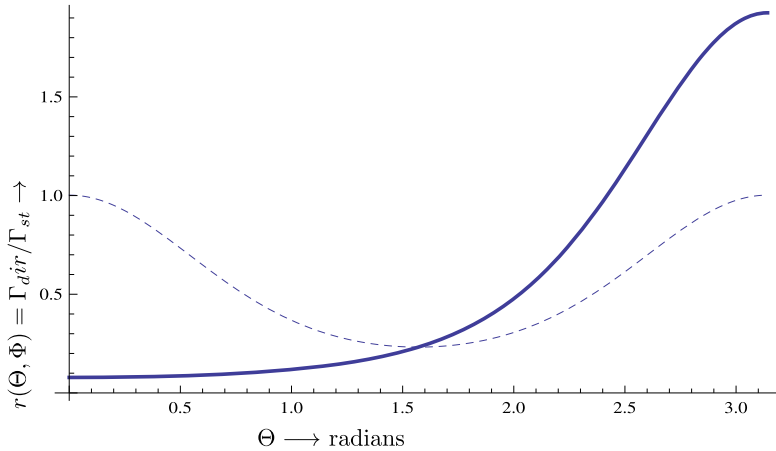


Fig. 5. The ratio of the width expected in a directional experiment divided by that expected in a standard experiment. The solid line is expected, if the sense of direction is known, while the dotted will show up, if the sense of direction is not known.

#### 4. The diurnal variation in directional experiments

The apparatus will be oriented in a direction specified in the local frame, e.g. by a point in the sky specified, in the equatorial system, by right ascension  $\tilde{\alpha}$  and inclination  $\tilde{\delta}$ .<sup>4</sup> This will lead to a diurnal variation<sup>5</sup> of the event rate [28]. This situation has already been discussed in the case of standard WIMPs [29]. We will briefly discuss the transformation into the relevant astronomical coordinates here.

The galactic frame, in the so called J2000 system, is defined by the galactic pole with ascension  $\tilde{\alpha}_1 = 12^h 51^m 26.282^s$  and inclination  $\tilde{\delta}_1 = +27^\circ 7' 42.01''$  and the galactic center at  $\tilde{\alpha}_2 = 17^h 45^m 37.224^s$ ,  $\tilde{\delta}_2 = -(28^\circ 56' 10.23'')$ . Thus the galactic unit vector  $\hat{y}$ , specified by  $(\tilde{\alpha}_1, \tilde{\delta}_1)$ , and the unit vector  $\hat{s}$ , specified by  $(\tilde{\alpha}_2, \tilde{\delta}_2)$ , can be expressed in terms of the celestial unit vectors  $\hat{i}$  (beginning of measuring the right ascension),  $\hat{k}$  (the axis of the Earth’s rotation) and  $\hat{j} = \hat{k} \times \hat{i}$ . One finds

$$\begin{aligned} \hat{y} &= -0.868\hat{i} - 0.198\hat{j} + 0.456\hat{k} \text{ (galactic axis),} \\ \hat{x} &= -\hat{s} = 0.055\hat{i} + 0.873\hat{j} + 0.483\hat{k} \text{ (radially out to the sun),} \\ \hat{z} &= \hat{x} \times \hat{y} = 0.494\hat{i} - 0.445\hat{j} + 0.747\hat{k} \text{ (sun’s velocity).} \end{aligned} \tag{4.13}$$

Note in our system the  $x$ -axis is opposite to the  $s$ -axis used by the astronomers. Thus a vector oriented by  $(\tilde{\alpha}, \tilde{\delta})$  in the laboratory is given in the galactic frame by a unit vector with components:

$$\begin{pmatrix} y \\ x \\ z \end{pmatrix} = \begin{pmatrix} -0.868 \cos \tilde{\alpha} \cos \tilde{\delta} - 0.198 \sin \tilde{\alpha} \cos \tilde{\delta} + 0.456 \sin \tilde{\delta} \\ 0.055 \cos \tilde{\alpha} \cos \tilde{\delta} + 0.873 \sin \tilde{\alpha} \cos \tilde{\delta} + 0.4831 \sin \tilde{\delta} \\ 0.494 \cos \tilde{\alpha} \cos \tilde{\delta} - 0.445 \sin \tilde{\alpha} \cos \tilde{\delta} + 0.747 \sin \tilde{\delta} \end{pmatrix}. \tag{4.14}$$

<sup>4</sup> We have chosen to adopt the notation  $\tilde{\alpha}$  and  $\tilde{\delta}$  instead of the standard notation  $\alpha$  and  $\delta$  employed by the astronomers to avoid possible confusion stemming from the fact that  $\alpha$  is usually used to designate the phase of the Earth and  $\delta$  for the ratio of the rotational velocity of the Earth around the Sun by the velocity of the sun around the center of the galaxy.

<sup>5</sup> This should not be confused with the diurnal variation expected even in non-directional experiments due to the rotational velocity of the Earth, which is expected to be too small.

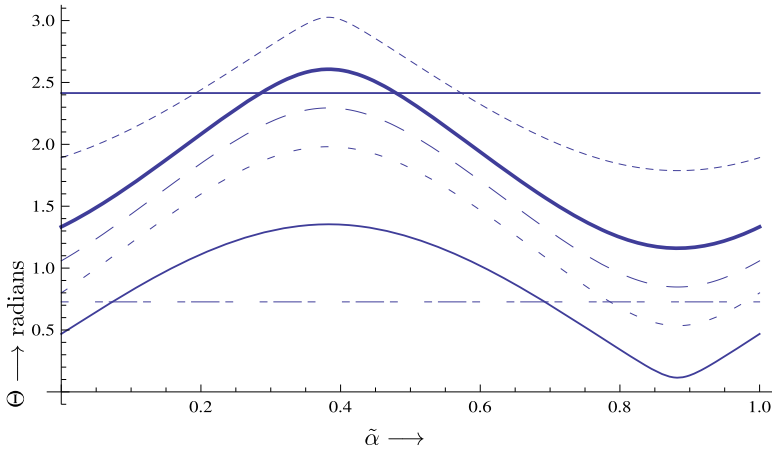


Fig. 6. Due to the diurnal motion of the Earth different angles  $\Theta$  in galactic coordinates are sampled as the earth rotates. The angle  $\Theta$  scanned by the direction of observation is shown for various inclinations  $\tilde{\delta}$ . We see that, for negative inclinations, the angle  $\Theta$  can take values near  $\pi$ , i.e. opposite to the direction of the sun’s velocity, where the rate attains its maximum. For an explanation of the curves see Fig. 7.

This can also be parametrized as:

$$x = \cos \gamma \cos \tilde{\delta} \cos (\tilde{\alpha} - \tilde{\alpha}_0) - \sin \gamma \left( \cos \tilde{\delta} \cos \theta_P \sin (\tilde{\alpha} - \tilde{\alpha}_0) + \sin \tilde{\delta} \sin \theta_P \right), \tag{4.15}$$

$$y = \cos (\theta_P) \sin \tilde{\delta} - \cos \tilde{\delta} \sin (\tilde{\alpha} - \tilde{\alpha}_0) \sin \theta_P, \tag{4.16}$$

$$z = \cos \delta \cos (\tilde{\alpha} - \tilde{\alpha}_0) \sin \gamma + \cos \gamma \left( \cos \tilde{\delta} \cos \theta_P \sin (\tilde{\alpha} - \tilde{\alpha}_0) + \sin \tilde{\delta} \sin \theta_P \right), \tag{4.17}$$

where  $\tilde{\alpha}_0 = 282.25^\circ$  is the right ascension of the equinox,  $\gamma \approx 33^\circ$  was given above and  $\theta_P = 62.6^\circ$  is the angle the Earth’s north pole forms with the axis of the galaxy.

Due to the Earth’s rotation the unit vector  $(x, y, z)$ , with a suitable choice of the initial time,  $\tilde{\alpha} - \tilde{\alpha}_0 = 2\pi(t/T)$ , is changing as a function of time

$$x = \cos \gamma \cos \tilde{\delta} \cos \left( \frac{2\pi t}{T} \right) - \sin \gamma \left( \cos \delta \cos \theta_P \sin \left( \frac{2\pi t}{T} \right) + \sin \tilde{\delta} \sin \theta_P \right), \tag{4.18}$$

$$y = \cos (\theta_P) \sin \tilde{\delta} - \cos \tilde{\delta} \sin \left( \frac{2\pi t}{T} \right) \sin \theta_P, \tag{4.19}$$

$$z = \cos \left( \frac{2\pi t}{T} \right) \cos \tilde{\delta} \sin \gamma + \cos \gamma \left( \cos \tilde{\delta} \cos \theta_P \sin \left( \frac{2\pi t}{T} \right) + \sin \tilde{\delta} \sin \theta_P \right), \tag{4.20}$$

where  $T$  is the period of the Earth’s rotation.

Some points of interest are:

The celestial pole:

$$(y, x, z) = (0.460, 0.484, 0.745) \Rightarrow (\theta = 62.6^\circ, \phi = 57^\circ),$$

The ecliptic pole:

$$(y, x, z) = (0.497, 0.096, 0.863) \Rightarrow (\theta = 62.6^\circ, \phi = 83.7^\circ),$$

The equinox:

$$(y, x, z) = (-0.868, 0.055, 0.494) \Rightarrow (\theta = 150.2^\circ, \phi = 83.7^\circ), \tag{4.21}$$



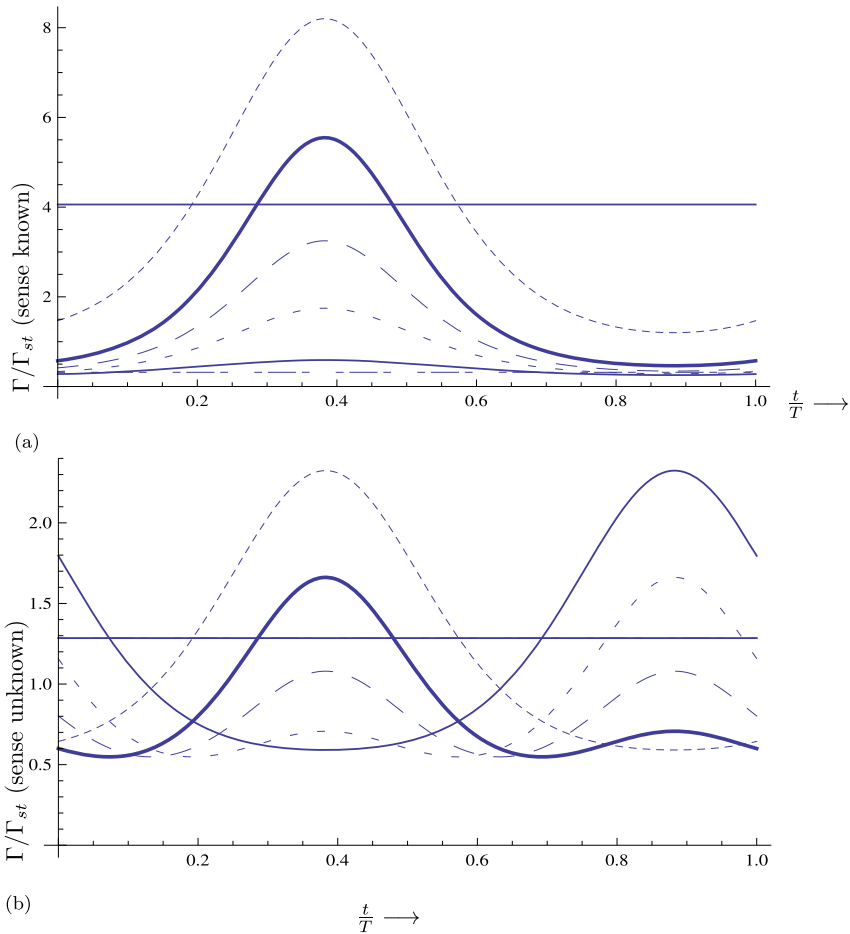


Fig. 7. The time dependence (in units of the Earth’s rotation period) of the ratio of the directional width divided by the non-directional width for various inclinations  $\tilde{\delta}$ , when the sense can be determined (a) or both senses are included (b). In The curves indicated by intermediate thickness solid, the short dash, thick solid line, long dashed, dashed, fine solid line, and the long–short dashed correspond to inclination  $\tilde{\delta} = -\pi/2, -3\pi/10, -\pi/10, 0, \pi/10, 3\pi/10$  and  $\pi/2$  respectively. We see that, for negative inclinations, the angle  $\Theta$  can take values near  $\pi$ , i.e. opposite to the direction of the sun’s velocity, where the rate attains its maximum if the sense of direction is known. There is no time variation, of course, when  $\tilde{\delta} = \pm\pi/2$ .

where  $\theta$  is defined with respect to the polar axis (here  $y$ ) and  $\phi$  is measured from the  $x$  axis towards the  $z$  axes.

Thus the angles  $\Theta$ , which is of interest to us in directional experiments, is given by

$$\Theta = \cos^{-1} z. \tag{4.22}$$

An analogous, albeit a bit more complicated expression can be derived for the angle  $\Phi$ .

The angle  $\Theta$  scanned by the direction of observation is shown, for various inclinations  $\tilde{\delta}$ , in Fig. 6. We see that for negative inclinations, the angle  $\Theta$  can take values near  $\pi$ , i.e. opposite to the direction of the sun’s velocity, where the rate attains its maximum (see Fig. 6).

The equipment scans different parts of the galactic sky, i.e. observes different angles  $\Theta$ . So the rate will change with time depending on whether the sense of observation. We assume that the sense of direction can be distinguished in the experiment. The total flux is exhibited in Fig. 7.

## 5. Discussion

In the present work we discussed the time variation of the width of the axion to photon resonance cavities involved in Axion Dark Matter Searches. We find two important signatures:

- Annual variation due to the motion of the Earth around the sun. We find that in the relative width, i.e. the width divided by its time average, can attain differences of about 15% between the maximum expected in June and the minimum expected six months later. This variation is larger than the modulation expected in ordinary dark matter of WIMPs. It does not depend on the geometry of the cavity or other details of the apparatus. It does not depend strongly on the assumed velocity distribution.
- A characteristic diurnal variation in of the width in directional experiments with most favorable scenario in the range of  $m_e L = 1.0\text{--}2.5 \times 10^{-3}$  eV m. This arises from asymmetries of the local axion velocity with respect to the sun's direction of motion manifested in a time dependent way due to the rotation of the Earth around its own axis. Admittedly such experiments are much harder, but the expected signature persists, even if one cannot tell the direction of motion of the axion velocity entering in the expression of the width. Anyway once such a device is operating, data can be taken as usual. Only one has to bin them according the time they were obtained. If a potentially useful signal is found, a complete analysis can be done according the directionality to firmly establish that the signal is due to the axion.

In conclusion in this work we have elaborated on two signatures that might aid the analysis of axion dark matter searches.

## Acknowledgements

One of the authors (JDV) is indebted to Professor J.E. Kim for useful discussions and to Leslie Rosenberg for his careful reading of the manuscript and his useful comments on directional experiments. IBS-Korea partially supported this project under system code IBS-R017-D1-2014-a00.

## References

- [1] R. Peccei, H. Quinn, *Phys. Rev. Lett.* 38 (1977) 1440.
- [2] S. Weinberg, *Phys. Rev. Lett.* 40 (1978) 223.
- [3] F. Wilczek, *Phys. Rev. Lett.* 40 (1978) 279.
- [4] J. Preskill, M.B. Wise, F. Wilczek, *Phys. Lett. B* 120 (1983) 127.
- [5] L.F. Abbott, P. Sikivie, *Phys. Lett. B* 120 (1983) 133.
- [6] M. Dine, W. Fischler, *Phys. Lett. B* 120 (1983) 137.
- [7] J. Primack, D. Seckel, B. Sadoulet, *Annu. Rev. Nucl. Part. Sci.* 38 (1988) 751.
- [8] P. Sikivie, *Phys. Rev. Lett.* 51 (1983) 1415.
- [9] I.P. Stern, on behalf of ADMX and ADMX-HF Collaborations, Axion dark matter searches, arXiv:1403.5332 [physics.ins-det], 2014.
- [10] G. Rybka, The axion dark matter experiment, in: IBS MultiDark Joint Focus Program WIMPs and Axions, Daejeon, S. Korea, October 2014.

- [11] S.J. Asztalos, et al., the ADMX Collaboration, Phys. Rev. Lett. 104 (2010) 041301, arXiv:0910.5914 [astro-ph.CO].
- [12] A. Wagner, et al., Phys. Rev. Lett. 105 (2010) 171801, for the ADMX collaboration, arXiv:1007.3766.
- [13] Center for Axion and Precision Physics research (CAPP), Daejeon 305-701, Republic of Korea, More information is available at [http://capp.ibs.re.kr/html/capp\\_en/](http://capp.ibs.re.kr/html/capp_en/).
- [14] S.J. Asztalos, et al., Nucl. Instrum. Methods Phys. Res. A 656 (2011) 39, arXiv:1105.4203 [physics.ins-det], 2014.
- [15] G. Raffelt, Astrophysical axion bounds, in: IBS MultiDark Joint Focus Program WIMPs and Axions, Daejeon, S. Korea, October 2014.
- [16] J. Hong, J.E. Kim, S. Nam, Y. Semertzidis, Calculations of resonance enhancement factor in axion-search tube experiments, arXiv:1403.1576 [hep-ph], 2014.
- [17] J.E. Kim, Phys. Rev. D 58 (1998) 055006.
- [18] L. Krauss, J. Moody, F. Wilczek, D. Morris, Phys. Rev. Lett. 55 (1985) 1797.
- [19] T.M. Shokair, et al., Future directions in microwave search for dark matter axions, Int. J. Mod. Phys. A 29 (2014) 1443004, <http://dx.doi.org/10.1142/S0217751X14430040>, arXiv:1405.3685 [physics.ins-det].
- [20] I.G. Irastorza, J.A. García, J. Cosmol. Astropart. Phys. 1210 (2012) 022, arXiv:1007.3766 [astro-ph.IM].
- [21] A.K. Drukier, K. Freese, D.N. Spergel, Phys. Rev. D 33 (1986) 3495.
- [22] M. Turner, Phys. Rev. D 42 (1990) 3572.
- [23] J. Vergados, Phys. Rev. D 85 (2012) 123502, arXiv:1202.3105 [hep-ph].
- [24] M. Kuhlen, M. Lisanti, D. Spergel, Phys. Rev. D 86 (2002) 063505, arXiv:1202.0007 [astro-ph.GA].
- [25] P. Sikivie, Phys. Lett. B 695 (2011) 22.
- [26] A.H. Guth, M.P. Hertzberg, C. Prescond-Weistein, arXiv:1412.5930 [astro-ph.CO].
- [27] J.D. Vergados, Phys. Rev. D 63 (2001) 063511.
- [28] S. Ahlen, The case for a directional dark matter detector and the status of current experimental efforts, in: J.B.R. Battat (Ed.), Int. J. Mod. Phys. A 25 (2001) 1, arXiv:0911.0323 [astro-ph.CO].
- [29] J.D. Vergados, C.C. Moustakidis, Eur. J. Phys. 9 (3) (2011) 628, arXiv:0912.3121 [astro-ph.CO].